Journal of Marine Research, 73, 49–69, 2015

Sandy sediment budget of the midcoast of Rio Grande do Sul, Brazil

by Lucas Marchi da Motta[1,2], Elírio Ernestino Toldo Jr.[1], Luiz Emílio de Sá Brito de Almeida[1], and José Carlos Nunes[1]

ABSTRACT

Calculation of the coastal sediment budget involves estimation of the timing and intensity of processes of erosion, transport, and deposition, as well as an understanding of local and regional sediment dynamics. The modern sedimentary deposits present in the coastal zone constitute the physical basis of coastal ecosystems. Knowledge of the dynamics of these sediments from the source to sink area, through regional sediment management, is critical to understanding the long-term stability of the coastal zone and the fate of these important natural resources. In this article, the littoral cell concept has been applied to the midcoast of Rio Grande do Sul, a wave-dominated and dissipative-intermediate sandy coast in southern Brazil. To analyze littoral drift variations along the 275 km long study area, the shoreline was divided into 12 cells. Littoral drift rates were estimated and compared using the energy flux method. Wave parameters were obtained from WAVEWATCH III. The sand volume of the coastal dune field (4.20 billion m^3) was quantified using satellite imagery and the aeolian transport rates estimated utilizing the sediment budget residual. The net annual longshore transport rates obtained with the Coastal Engineering Research Center equation range from 0.60 to 2.63 million m^3 per year. The littoral drift rates obtained with the Van Rijn (2001) and Kamphuis (1991) equations range between 0.15 and 1.00 million m^3 per year. Based on the sediment budget and dune field age, the CERC formula seems more appropriate to estimate longshore transport.

Keywords. Longshore sediment transport, nearshore dynamics, dunes, beach erosion

1. Introduction

Calculation of the coastal sediment budget provides an estimate of the time and intensity of processes associated with erosion, transport, and deposition and aids in the understanding of local and regional sediment dynamics applied, for instance, to the mapping of risk areas. The modern sedimentary deposits present in the coastal zone constitute the physical basis of coastal ecosystems. Knowledge of the dynamics of these sediments from the source to

1. Instituto de Geociências of Universidade Federal do Rio Grande do Sul (UFRGS), Av. Bento Gonçalves 9500, bairro Agronomia. Porto Alegre, Rio Grande do Sul, Brasil
2. Corresponding author ***e-mail: lucas.motta@ufrgs.br***

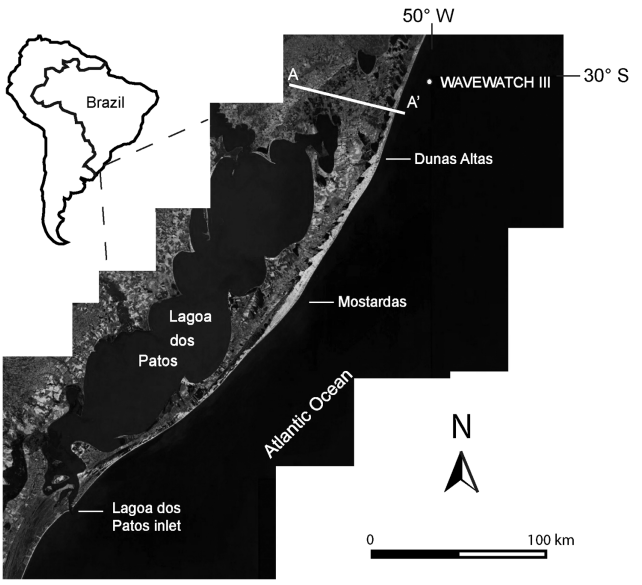

Figure 1. Location of the midcoast between Lagoa dos Patos inlet and Dunas Altas beach, a 275 km long Holocene fine sand barrier and the point to collect wave data from the WAVEWATCH III.

sink area, through regional sediment management, is critical to understanding the long-term stability of the coastal zone and the fate of these important natural resources. On a yearly to decadal scale, sediment supply to a beach can be defined as the volume of sediment contained within and moving along it. According to Rosati (2005), a sediment budget represents the addition and removal of sediments within a defined time interval and area. Bowen and Inman (1966) developed the concept of a sediment budget to identify and quantify sandy sediment sources and sinks on California beaches, dividing the area of interest into littoral cells and subcells. Since then, several studies have been conducted on different beaches using this concept, such as Patsch and Griggs (2008) in California; Rodríguez and Dean (2009) in Florida; Cooper, Hooke, and Bray (2001) in southern England; Anthony, Vanhee, and Ruz (2006) in northern France; and Frihy and Dewidar (2003) on the Nile River delta.

In this article, we develop a sediment budget for the wave-dominated sandy midcoast of Rio Grande do Sul (RS), southern Brazil (Fig. 1), during the period from 1998 to 2009, through the division of 275 km of coastline into cells.

2. Study area

The RS coastal plain, which covers approximately 33,000 km^2, consists of four barrier-lagoon–type depositional systems associated with cycles of glacio-eustatic sea-level

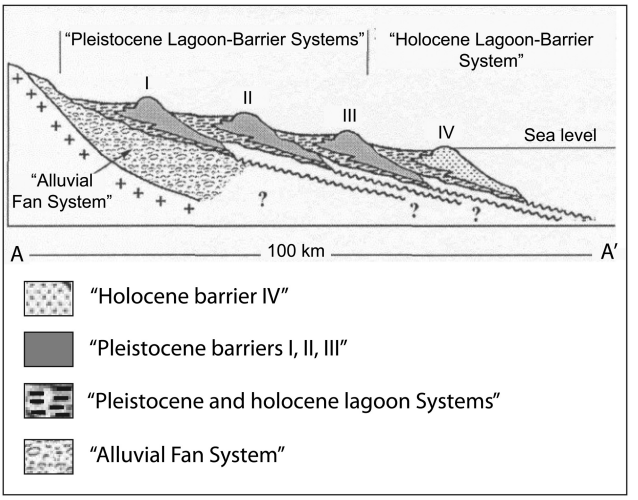

Figure 2. Stratigraphic details of barrier-lagoon systems I, II, III, and IV from cross section A–A′ (Fig. 1). Modified from Tomazelli et al. (2000).

variations that occurred during the Quaternary, and they mark the transgressive maxima of each event (Tomazelli, Dillenburg, and Villwock 2000). These deposits have been termed, from oldest to youngest, as barriers I, II, III, and IV. Each barrier complex consists of lagoonal, aeolian, beach, and marine facies with a northeast to southwest orientation. They developed over the past 400 ka, associated with the last four transgressive-regressive events. The first three barriers are of Pleistocene age, and the most recent, barrier IV, was formed during the Holocene (Fig. 2). This study is concerned with the 275 km long stretch of coast between Lagoa dos Patos inlet and Dunas Altas beach (Fig. 1).

The Holocene barrier beach is slightly sinuous along its 615 km length (Fig. 1). Dillenburg et al. (2006) studied the stratigraphic evolution of barrier IV using aerial photographs, boreholes, and ^{14}C dating. These authors identified two main lithofacies composed of aeolian sand overlying beach sands. Well-preserved marine mollusks of *Olivanicillaria urceus*, *Mactra* sp., and *Donax* sp. in the beach sands have been dated between 7 and 8 ka. This age is used to mark the beginning of Holocene barrier accumulation and development of the coastal dune field. Aeolian deposits of fine quartz sand occupy virtually the entire surface of the Holocene barrier (Fig. 1). The adjacent continental shelf is between 150 and 200 km wide, reaching maximum depths of approximately 100 to 140 m, with slopes ranging from 0.5 to 1.5 m km^{-1} (Corrêa 1996). The coastline is dominated by waves (Jung and Toldo 2011; Toldo et al. 2013), and regional processes of erosion and deposition are primarily controlled by wave energy flux parallel to the beach (Lima, Almeida, and Toldo 2001; Toldo et al. 2006).

a. Beaches

The RS coast receives no modern sand contributions from the mainland because the entire bed load of the drainage network is retained in the lagoons of Lagoa dos Patos and Lagoa Mirim (Tomazelli et al. 1998; Toldo et al. 2000). Thus, the most important control on the beach sediment budget on a short-term timescale is littoral drift, which is mainly forced by incident waves. The beach sediment has a uniform grain size (Median grain size is 0.15 mm) and consists mainly of quartz with low carbonate contents (between 0.2% and 0.5%). The concentration of heavy minerals varies widely, locally reaching values of up to 40% north of the Lagoa dos Patos inlet (Toldo et al. 2006).

The coast is characterized by intermediate and dissipative beaches, following the classification of Wright and Short (1984), although some sectors are temporarily reflective (Calliari, Toldo, and Nicolodi 2006). Stretches of coast with erosional tendencies have steep slopes and scarps in the berm and/or foredune. Stable stretches comprise gently sloping, large subaerial beaches with cusps and well-developed frontal dunes. Tomazelli et al. (2000) associated the height of the frontal dunes in the north and midcoast of RS with incidence of northeast winds, the most frequent winds on the coast. High dunes at Mostardas and Dunas Altas are attributed to the large angle between the beach and prevailing northeast winds.

b. Hydrodynamics

Incident waves have a seasonal behavior. Strong waves generated from the South Atlantic Ocean occur in fall and winter and are associated with the passage of cold fronts. During the spring and summer, waves are generated by strong local northeast winds. Significant height is 1.5 m with periods between 7 and 9 s. The astronomical tide is semidiurnal and has mean amplitude of 0.25 m, and the meteorological tide amplitude can reach 1.20 m. Based on two wave data sets for the period 1963 to 1996 on the northern coast of RS, the depth of closure on the shoreface has been estimated at 7.5 m (Almeida et al. 1999).

The directional distribution of the longshore current throughout the entire coast is from the southwest and northeast, in a clearly bidirectional pattern. However, sediment transport associated with southwest longshore currents is more vigorous than that originating from the northeast because southwest currents mostly result from greater wave energy flux associated with the passage of cold fronts (Lima, Almeida, and Toldo 2001).

3. Methods

a. Littoral cells

Based on the littoral cell concept proposed by Bowen and Inman (1966) and modified by the U.S. Army Coastal Engineering Research Center (1984); Cooper, Hooke, and Bray (2001); Rosati and Kraus (2001); Frihy and Dewidar (2003); Rosati (2005); Anthony, Vanhee, and Ruz (2006); Patsch and Griggs (2008); and Rodríguez and Dean (2009), morphological limits were established along the midcoast. Cells were identified along the 275

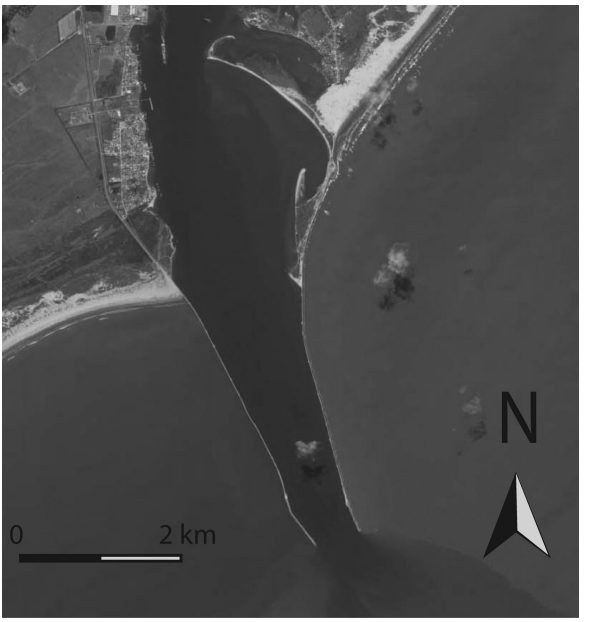

Figure 3. Landsat image of the Lagoa dos Patos inlet, fixed by the construction of jetties in 1914.

Table 1. Orientation (azimuth) and the length of the cells.

Cell	1	2	3	4	5	6	7	8	9	10	11	12
Angle (°)	40.3	54.7	56.5	48.7	40.6	46.0	39.7	29.4	32.0	33.3	25.4	18.4
Length (km)	24.8	17.2	28.7	30.0	26.2	21.0	20.5	21.5	40.9	14.9	13.1	19.6

km long beach system from the Lagoa dos Patos inlet to the Dunas Altas beach (Fig. 1). The mouth of the lagoon has been fixed since the beginning of the 20th century by two large jetties that extend more than 4 km into the sea and represent a major obstacle to sand transfer between the mid- and south coasts of RS (Fig. 3). The geomorphological criterion used to establish the northeast boundary of the littoral cell is associated with significant size reduction of the coastal dune field. Urbanized areas are concentrated in this location. The onshore and offshore boundaries of the littoral cell, or the coastal and seaward limit of the beach profile change, were established between the foot of the frontal dune and the inferred depth of closure.

Although small in magnitude, changes in shoreline orientation were used as topographic geoindicators for the division of 12 littoral cells (Table 1). The orientation angle of each alignment (azimuth) was defined trigonometrically based on the Universal Transverse Mercator X and Y point coordinates (Fig. 4).

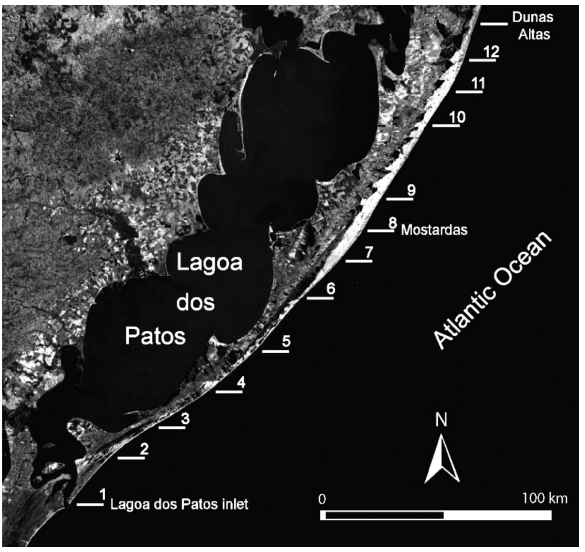

Figure 4. Coastal dune field surface (white area) along the midcoast and coastline morphological details surrounding the 12 cells.

b. Sediment budget

The greatest challenge in developing a sediment budget is identifying sand sources and sinks and quantifying the transport rates into and out of each littoral cell (Patsch and Griggs 2008). The absence of a long time series of wave measurements along the coast is also a major source of uncertainty in the calculation of the directional distribution of energy flux and, consequently, the sediment budget. Another difficulty, which leads to an increase in the inaccuracy of this calculation, is the lack of periodic topographic surveys of the beach profile.

Earlier work by Toldo et al. (2006) identified no source of sediments to the sediment budget other than erosion of the beach system itself. However, at the Holocene timescale Dillenburg et al. (2000) observed that the continental shelf is an important source of sediment to the beach through onshore transport. However, this transport mechanism was not considered in the calculation of the sediment budget because of the timescale considered. Parameters controlling the sediment budget were defined by the transport mechanism and its capacity to transport sediment into or out of each cell (Table 2).

Based on the concept developed by Bowen and Inman (1966) according to which the sandy sediment budget involves the principle of conservation of mass, the balance was assessed for each cell for the period 1998–2009 applying the methodology of Rosati and Kraus (2001) (Fig. 5).

Table 2. Transport mechanisms applied to the sediment budget, proposed by Toldo et al. (2006, 2013).

Addition	Removal
Littoral drift	Littoral drift
Aeolian transport	Aeolian transport
Washouts	Coastal jet

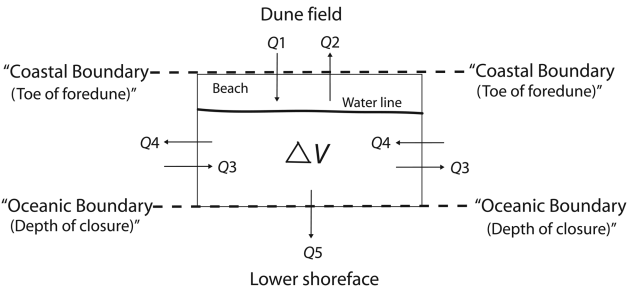

Figure 5. General diagram for calculating the sediment budget applied to the littoral cells, where $Q1$ is addition by wind and washouts, $Q2$ is removal by wind, $Q3$ is addition and removal by southwest littoral drift, $Q4$ is addition and removal by northeast littoral drift, $Q5$ is removal by coastal jet, and ΔV is change in volume within the cell. Adapted from Rosati and Kraus (2001).

i. Littoral drift. Littoral drift is the main controlling variable of the sediment budget on the midcoast of RS because of the magnitude of the wave energy flux compared with other forces, such as wind and tides. It is notoriously difficult to measure or model longshore drift, and all existing methods are subject to severe limitations (Cooper and Pilkey 2004). Wave parameters used to estimate littoral drift rates were taken from the NOAA WAVEWATCH III (NWW3) operational model hindcast reanalysis (Tolman 1997, 1999) from a site located north of the midcoast (Fig. 1). The period, significant height, and peak direction were continually modeled in deep water at 3-hour intervals between 1998 and 2009 and accounted for more than 35,000 records. The data from the WAVEWATCH III model were transferred to break point conditions using linear wave theory according to the methodology of Herbich (2000).

Sand transport by longshore currents was calculated using three methods, including (1) the Coastal Engineering Research Center (CERC) formula, (2) Van Rijn (2001), and (3) Kamphuis (1991), as follows:

$$Q = 0.025\ H_r^2 \sqrt{g\, d}_r\ \sin(2\alpha_r), \tag{1}$$

where Q is the volume of transported sediments ($m^3\ s^{-1}$); H_r and d_r correspond to the wave height and depth at break point (m), respectively; α_r is the wave incidence direction (°); and g is the acceleration attributable to gravity ($m\ s^{-2}$).

$$Q = 40\ {H_r}^3 \sin(2\alpha_r), \tag{2}$$

where Q is the transported volume in kg s^{-1} and H_r is the wave height at break point (m).

$$Q = 2.33(T)^{1.5}\ (\tan\beta)^{0.75}(d_{50})^{(-0.25)}(H_r)^2[\sin(2\alpha_r)]^2 \quad (3)$$

where Q is the transported volume in kg s^{-1}, T is the period (s), tan β is the beach slope, and d_{50} is the median grain size (meter).

These equations have been widely used in academic and coastal engineering studies (Kamphuis 1991; Van Rijn 2001, 2002; Van Rijn and Boer 2006). The three methodologies were used to calculate annual littoral drift volumes for each cell based on the same wave parameter records from the WAVEWATCH III model.

ii. Washouts. Washouts (channels cut in the beach during high runoff) add sediments by moving sand from the dunes into the littoral cells. However, because of the lack of information on the volume of this mechanism of the sediment supply, this component was not considered in the budget. Figueiredo and Calliari (2006) have defined and mapped the presence of washouts along the midcoast of RS and observed the highest occurrence near the Lagoa dos Patos inlet and between the Mostardas and Dunas Altas beaches. The authors concluded that the presence of washouts was not linked to the prevalence of erosive or depositional processes on the beach system but was a result of the geological and geomorphological components of the adjacent coastal plain. In addition, they identified seasonal control in the washouts, occurring more and less frequently during winter and summer, respectively, justified by the higher incidence of precipitation in winter and increased evaporation rates in summer.

iii. Coastal jet. Toldo et al. (2006) identified the development of a coastal jet associated with the passage of cold fronts on the Mostardas beach in cell 7. Analyses of satellite images in this area reveal the presence of a short-term coastal current circulation overtopping the shoreface. These currents have not been studied in detail, but it seems likely that in some instances this current can lead to enhanced diffusion of suspended sediment seaward from the surf zone (Fig. 6). A strong coastal jet characterizes this coastal current. The occurrence and evolution of this jet are closely related to the passage of cold fronts, which are formed early in the winter. The characteristics of the circulation pattern over the shoreface consisted of two segments, the northward coastal current intensified by the south and southeast winds and a wide plume behaving like a clockwise-rotating gyre from southeast to east-northeast. The conceptual model is that sediments are supplied to the surf zone and shoreface from shoreline erosion. A fraction of the suspended load is incorporated by the shoreface every year, developing a large sand bank as can be seen in the 10 m bathymetric contour, but there are no measurements or estimates of the remobilized sand volumes. Also, the physical processes that control the formation and evolution of the coastal jet have not been fully explored, but good agreement was found between the shoreface accretion area, for more than 2 km offshore, and the extension of the coastal jet over this area, as observed in the satellite image (Toldo et al. 2006).

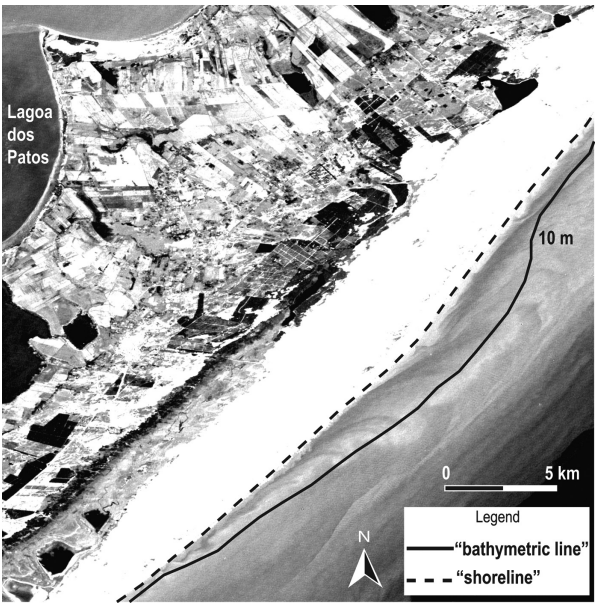

Figure 6. The satellite image shows the large extent of the coastal dune field (light color) surrounding the site with soft inflection in the beach line and the coastal jet along Mostardas beach. The plume is located between the shoreline and bathymetric line of 10 m, behaving like a clockwise-rotating gyre from southeast to east-northeast (Toldo et al. 2006).

iv. Aeolian transport. Aeolian transport causes a net landward transport of sand from the cells. There are no measurements that quantify the annual volume, but in this case, it was possible to evaluate the amount of sand contained in the dune field to estimate the transport rates and compare this with reservoir age.

To assess the amount of sediments in the dune field, the software Global Mapper 11 and a mosaic of Advanced Spaceborne Thermal Emission and Reflection Radiometer–Global Digital Elevation Model images were used, with a spatial resolution of 30 m and a vertical resolution of 1 m, superimposed on Landsat 7 images. Errors and inaccuracies of this methodology were established from a field planialtimetric survey conducted near the Dunas Altas beach, comparing the data obtained with the satellite image results. In the topographic measurement, a dune of approximately 30,000 m^2 was demarcated by a grid of 1,717 points, with planar coordinates and altitudes using the Topcon GR3 dual-frequency Differential Global Positioning System operated in kinematic mode. In the final adjustment, the coordinates were compared with those stored in the Rede Brasileira de Monitoramento Contínuo base station and followed by postprocessing. The Mapgeo 2010 software from Brazilian Institute of Geography and Statistics was used to correct the orthometric height. Maximum vertical and horizontal errors of 15.43 and 15 cm, respectively, were observed. A dune volume of 393,498.6 m^3 was calculated using Software Surfer 9 and 332,676.2 m^3

Hs (m)	N	NNE	NE	ENE	E	ESE	SE	SSE	S	SSW
<0.5			0.06	0.09	0.14	0.07	0.03	0.07	0.03	
0.5 - 1.0	0.03	0.12	1.02	4.61	3.41	1.95	1.55	2.02	1.25	0.21
1.0 - 1.5	0.01	0.06	2.39	6.51	7.80	4.86	3.64	6.22	4.27	0.85
1.5 - 2.0		0.01	1.02	4.39	3.98	3.21	3.20	7.02	3.58	0.86
2.0 - 2.5			0.15	1.25	1.31	1.37	1.75	3.77	1.51	0.31
2.5 - 3.0			0.01	0.19	0.40	0.56	0.71	1.31	0.41	0.09
3.0 - 3.5				0.01	0.10	0.11	0.18	0.41	0.15	0.04
3.5 - 4.0					0.03	0.05	0.06	0.06	0.03	0.01
4.0 - 4.5						0.01	0.01	0.02		
4.5 - 5.0						0.01				
5.0 - 5.5						0.01	0.01			
5.5 - 6.0						0.01				
TOTAL (%)	0.04	0.19	4.65	17.04	17.17	12.22	11.13	20.90	11.23	2.37

Figure 7. Wave regime from the WAVEWATCH III model, 1998–2009 period. E, east; ENE, east-northeast; ESE, east-southeast; N, north; NE, northeast; NNE, north-northeast; S, south; SE, south-east; SSE, south-southeast; SSW, south-southwest.

using Global Mapper 11, a difference of approximately 15% of topographic measurement and satellite images.

4. Results

a. Wave and littoral drift regime

Wave data for the midcoast of RS were generated from the WAVEWATCH III model. Waves from the south-southeast, east, and east-northeast were observed to be the most frequent, and the highest waves were from the east-southeast (Fig. 7).

The sediment volume annually transported between 1998 and 2009 ranged from 1.10 to 2.93 million m^3 to the northeast and between 0.60 and 2.41 million m^3 to the southwest, based on equation (1). Using equation (2), for the same period, the volume transported was between 0.35 and 1 million m^3 to the northeast and between 0.15 and 0.78 million m^3 to southwest. From equation (3), the transport ranged from 0.28 to 0.70 million m^3 to the northeast and from 0.10 to 0.47 million m^3 to the southwest. The results of annual longshore transport rates calculated between 1998 and 2009 applying the three equations are shown in Tables 3, 4, and 5, respectively.

An annual net drift to the northeast is markedly present in all cells. However, a reversal occurred in cells 2 and 3 in the years 1998, 2000, 2001, 2004, and 2008, all of which are in the southern half of the study area (Fig. 8). These two cells had the largest alignment angles (54° to 56°), whereas the other cells had values lower than 49°. Net littoral drift reversal also occurred in the year 2001.

b. Dune field volume

The coastal dune field consists of an extensive regional sand reservoir with no discontinuities between the cells. Considerable dune field widening occurred in the more pronounced

Table 3. Longshore transport rates ($\times 10^6$ m^3) between 1998 and 2009 for each cell applying CERC (equation 1). NE, northeast; SW, southwest.

Cell		1	2	3	4	5	6	7	8	9	10	11	12
2009	SW	1.54	1.60	1.60	1.58	1.54	1.57	1.53	1.40	1.45	1.47	1.31	1.12
	NE	2.45	1.81	1.69	2.14	2.45	2.26	2.47	2.53	2.55	2.55	2.46	2.26
2008	SW	2.26	2.41	2.41	2.37	2.26	2.35	2.24	1.93	2.02	2.06	1.79	1.50
	NE	2.21	1.70	1.62	1.94	2.21	2.05	2.23	2.37	2.34	2.32	2.40	2.41
2007	SW	0.98	1.02	1.04	1.00	0.98	0.99	0.98	0.99	0.99	0.99	0.99	1.00
	NE	2.57	2.11	2.01	2.39	2.57	2.47	2.58	2.48	2.53	2.55	2.37	2.14
2006	SW	1.28	1.30	1.32	1.28	1.28	1.28	1.29	1.28	1.29	1.29	1.24	1.13
	NE	2.77	1.93	1.79	2.35	2.76	2.51	2.79	2.92	2.93	2.92	2.86	2.61
2005	SW	1.33	1.47	1.48	1.44	1.33	1.41	1.31	1.11	1.16	1.19	1.05	0.97
	NE	2.33	1.82	1.71	2.11	2.33	2.21	2.34	2.29	2.33	2.34	2.24	2.15
2004	SW	1.87	2.07	2.07	2.01	1.88	1.97	1.86	1.63	1.70	1.73	1.51	1.29
	NE	1.95	1.45	1.37	1.70	1.95	1.79	1.97	2.13	2.11	2.09	2.14	2.13
2003	SW	0.60	0.73	0.77	0.64	0.60	0.61	0.60	0.63	0.62	0.62	0.65	0.67
	NE	2.48	1.92	1.82	2.21	2.47	2.32	2.49	2.49	2.52	2.53	2.40	2.15
2002	SW	1.01	0.88	0.88	0.92	1.00	0.95	1.01	1.06	1.06	1.05	1.05	0.99
	NE	2.18	1.60	1.50	1.91	2.17	2.02	2.19	2.18	2.21	2.22	2.09	1.85
2001	SW	1.85	1.72	1.69	1.82	1.85	1.84	1.84	1.70	1.75	1.78	1.61	1.37
	NE	1.46	1.16	1.10	1.33	1.46	1.38	1.47	1.49	1.49	1.49	1.48	1.45
2000	SW	1.18	1.53	1.57	1.39	1.19	1.32	1.17	1.06	1.07	1.08	1.05	1.01
	NE	1.82	1.40	1.33	1.62	1.82	1.70	1.84	2.05	2.01	1.98	2.12	2.16
1999	SW	1.63	1.32	1.29	1.45	1.62	1.51	1.64	1.76	1.75	1.74	1.75	1.67
	NE	2.26	1.73	1.62	2.03	2.26	2.13	2.27	2.24	2.28	2.29	2.15	1.93
1998	SW	1.64	1.51	1.50	1.55	1.63	1.58	1.64	1.66	1.67	1.67	1.64	1.54
	NE	1.85	1.31	1.22	1.56	1.84	1.67	1.87	1.99	1.98	1.97	1.98	1.91
Total	SW	17.1	17.5	17.6	17.4	17.1	17.3	17.1	16.2	16.5	16.6	15.6	14.2
	NE	26.3	19.9	18.7	23.2	26.2	24.5	26.5	27.1	27.2	27.2	26.6	25.1

shoreline inflections between cells 6–8 and 10–12 (Fig. 4). The dunes of cells 6–8 had the greatest sand volume with 2 billion m^3, followed by cells 10–12 with 837 million m^3, cell 9 with 743 million m^3, and cells 1–5 with 620 million m^3. The total volume of the dune field is 4.20 billion m^3, and almost half of this volume is found between cells 6 and 8.

c. Sediment budget

The sediment budget was calculated for each cell based on the littoral drift rates, both southwest and northeast, according to the diagram shown in Figure 5. In the budget for cell

Table 4. Longshore transport rates ($\times 10^6$ m^3) between 1998 and 2009 for each cell applying Van Rijn (2001) (equation 2). NE, northeast; SW, southwest.

Cell		1	2	3	4	5	6	7	8	9	10	11	12
2009	SW	0.45	0.48	0.48	0.47	0.45	0.47	0.45	0.41	0.42	0.43	0.38	0.31
	NE	0.84	0.63	0.59	0.74	0.84	0.78	0.84	0.84	0.85	0.86	0.80	0.71
2008	SW	0.70	0.78	0.78	0.75	0.71	0.74	0.70	0.59	0.62	0.63	0.55	0.46
	NE	0.73	0.57	0.54	0.65	0.73	0.68	0.74	0.78	0.77	0.76	0.79	0.80
2007	SW	0.27	0.29	0.30	0.28	0.27	0.27	0.27	0.26	0.26	0.26	0.26	0.26
	NE	0.87	0.72	0.69	0.82	0.87	0.84	0.87	0.80	0.83	0.84	0.76	0.66
2006	SW	0.35	0.38	0.39	0.36	0.35	0.36	0.35	0.35	0.35	0.35	0.34	0.31
	NE	0.97	0.68	0.63	0.83	0.96	0.88	0.97	0.99	1.00	1.00	0.96	0.85
2005	SW	0.40	0.47	0.47	0.45	0.40	0.43	0.39	0.31	0.33	0.34	0.28	0.26
	NE	0.76	0.60	0.57	0.70	0.76	0.73	0.76	0.72	0.74	0.75	0.70	0.67
2004	SW	0.56	0.64	0.64	0.61	0.56	0.60	0.56	0.47	0.50	0.51	0.43	0.36
	NE	0.66	0.49	0.47	0.58	0.66	0.61	0.66	0.71	0.70	0.70	0.70	0.69
2003	SW	0.15	0.21	0.22	0.17	0.15	0.16	0.15	0.16	0.15	0.15	0.16	0.17
	NE	0.81	0.64	0.60	0.73	0.80	0.76	0.81	0.79	0.80	0.81	0.75	0.65
2002	SW	0.27	0.23	0.24	0.24	0.26	0.25	0.27	0.28	0.28	0.28	0.28	0.27
	NE	0.73	0.53	0.49	0.64	0.73	0.68	0.73	0.71	0.73	0.73	0.67	0.58
2001	SW	0.54	0.51	0.50	0.54	0.55	0.54	0.55	0.50	0.52	0.53	0.48	0.41
	NE	0.46	0.38	0.35	0.43	0.46	0.44	0.47	0.47	0.47	0.47	0.46	0.45
2000	SW	0.34	0.47	0.49	0.42	0.34	0.39	0.33	0.29	0.29	0.30	0.28	0.27
	NE	0.59	0.46	0.43	0.52	0.59	0.55	0.59	0.65	0.64	0.63	0.67	0.68
1999	SW	0.45	0.37	0.36	0.40	0.45	0.42	0.45	0.49	0.49	0.48	0.49	0.47
	NE	0.76	0.59	0.55	0.69	0.76	0.72	0.76	0.73	0.75	0.76	0.69	0.61
1998	SW	0.47	0.44	0.44	0.45	0.47	0.46	0.47	0.48	0.48	0.48	0.47	0.44
	NE	0.59	0.42	0.40	0.51	0.59	0.54	0.60	0.62	0.63	0.63	0.62	0.58
Total	SW	4.95	5.27	5.31	5.14	4.96	5.09	4.94	4.59	4.69	4.74	4.40	3.99
	NE	8.77	6.71	6.31	7.84	8.75	8.21	8.80	8.81	8.91	8.94	8.57	7.93

12 (Fig. 4), in the extreme north of the midcoast, southwest drift rates of the shore segment to the north were included. However, for cell 1, the input of sediments coming from the south side of the Lagoa dos Patos inlet was considered insignificant because of the physical barrier represented by the Rio Grande jetties.

Cells 2, 3, 6, and 12 had positive sediment budgets throughout the period from 1998 to 2009 and were classified as sandy sediment sinks. Cells 1, 4, 5, 7, 10, and 11 showed negative budgets, being locations with a prevalence of erosion, and were classified as sediment sources. Cells 8 and 9 showed different behavior depending on the equation used, but the

Table 5. Longshore transport rates ($\times 10^6$ m^3) between 1998 and 2009 for each cell applying Kamphuis (1991) (equation 3). NE, northeast; SW, southwest.

Cell		1	2	3	4	5	6	7	8	9	10	11	12
2009	SW	0.28	0.32	0.32	0.30	0.28	0.29	0.28	0.25	0.26	0.26	0.23	0.19
	NE	0.61	0.49	0.47	0.55	0.61	0.57	0.61	0.62	0.62	0.63	0.60	0.55
2008	SW	0.41	0.47	0.47	0.44	0.41	0.43	0.40	0.33	0.35	0.36	0.31	0.26
	NE	0.55	0.43	0.41	0.48	0.55	0.51	0.55	0.59	0.58	0.57	0.59	0.59
2007	SW	0.19	0.21	0.21	0.20	0.19	0.20	0.19	0.18	0.18	0.19	0.17	0.16
	NE	0.62	0.53	0.51	0.59	0.62	0.60	0.62	0.59	0.60	0.61	0.56	0.52
2006	SW	0.25	0.30	0.30	0.27	0.25	0.26	0.24	0.23	0.23	0.23	0.22	0.20
	NE	0.67	0.50	0.47	0.59	0.67	0.62	0.67	0.70	0.70	0.70	0.69	0.63
2005	SW	0.26	0.29	0.29	0.28	0.26	0.27	0.26	0.20	0.22	0.23	0.18	0.16
	NE	0.55	0.46	0.44	0.52	0.55	0.53	0.55	0.54	0.55	0.55	0.54	0.52
2004	SW	0.34	0.40	0.40	0.39	0.34	0.37	0.34	0.30	0.31	0.32	0.27	0.22
	NE	0.50	0.39	0.37	0.44	0.49	0.46	0.50	0.53	0.53	0.53	0.53	0.51
2003	SW	0.12	0.18	0.19	0.15	0.12	0.14	0.12	0.11	0.11	0.11	0.11	0.10
	NE	0.60	0.48	0.46	0.54	0.60	0.57	0.60	0.60	0.61	0.61	0.58	0.53
2002	SW	0.19	0.18	0.19	0.18	0.19	0.18	0.19	0.19	0.19	0.19	0.19	0.18
	NE	0.54	0.43	0.40	0.49	0.54	0.52	0.55	0.53	0.54	0.55	0.51	0.46
2001	SW	0.34	0.33	0.33	0.35	0.34	0.35	0.34	0.31	0.32	0.33	0.29	0.25
	NE	0.34	0.29	0.28	0.32	0.34	0.33	0.34	0.35	0.35	0.34	0.35	0.34
2000	SW	0.22	0.30	0.30	0.27	0.22	0.26	0.22	0.18	0.19	0.19	0.17	0.16
	NE	0.44	0.36	0.34	0.40	0.44	0.42	0.44	0.49	0.48	0.47	0.50	0.48
1999	SW	0.28	0.26	0.26	0.27	0.28	0.27	0.28	0.28	0.28	0.28	0.28	0.26
	NE	0.52	0.43	0.41	0.48	0.52	0.50	0.52	0.51	0.52	0.53	0.49	0.45
1998	SW	0.28	0.28	0.28	0.28	0.28	0.28	0.28	0.26	0.27	0.27	0.26	0.24
	NE	0.41	0.31	0.29	0.36	0.41	0.38	0.42	0.43	0.43	0.43	0.43	0.41
Total	SW	3.16	3.52	3.54	3.38	3.16	3.30	3.14	2.82	2.91	2.96	2.68	2.38
	NE	6.35	5.10	4.85	5.76	6.34	6.01	6.37	6.48	6.51	6.52	6.37	5.99

volume variation was very small, which demonstrated the stability in balance of these cells (Table 6).

The sediment budget results showed alternating erosional and depositional trends in the same cell depending on the season of the year, mainly in cells 7, 8, 9, 10, and 11 (Table 7), located between the two largest shoreline inflections on the Mostardas and Dunas Altas beaches. This information revealed that the regional sediment budget is also controlled by the seasonality of wave parameters, causing changes in the classification of cells from sandy sediment sources to sinks according to season. Thus, it was concluded that the coastal dynamics in these locations were more complex than in other cells that did not show seasonal variation.

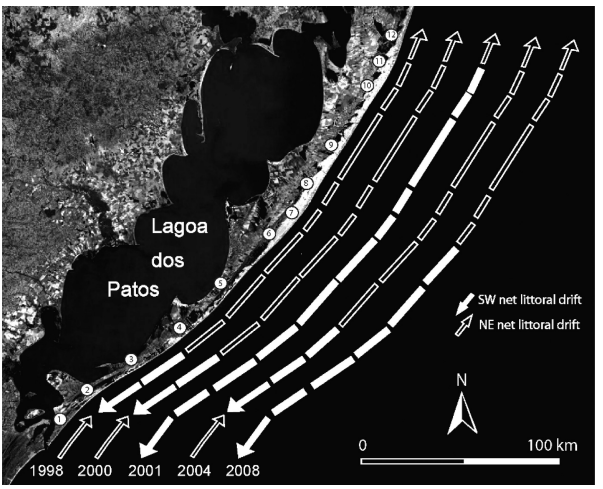

Figure 8. Net littoral drift for each cell for the years 1998, 2000, 2001, 2004, and 2008. The northeast direction is dominant but reversals are prevalent in the southern part of the study area. In 2001, reversal occurred along almost the entire coast. NE, northeast; SW, southwest.

Table 6. Sediment erosion (−) and deposition (+) volumes in each cell ($\times 10^6 m^3$) calculated from the longshore drift rates, 1998–2009 period.

Cell	1	2	3	4	5	6	7	8	9	10	11	12
Equation (1)	−8.8	6.5	0.98	−4.8	−2.8	1.5	−2.9	−0.38	0.02	−1	−0.8	2.3
Equation (2)	−3.5	2.1	0.2	−1.7	−0.8	0.4	−0.9	0.08	−0.04	−0.4	−0.05	0.9
Equation (3)	−2.8	1.3	0.08	−1.1	−0.4	0.2	−0.7	−0.03	0.09	−0.3	−0.1	0.7

Table 7. Tendency of coastline erosion (−) and deposition (+) in each cell related to season, 1998–2009 period.

Cell	1	2	3	4	5	6	7	8	9	10	11	12
Autumn	−	+	−	−	−	+	−	−	+	−	−	+
Winter	−	+	+	−	−	+	−	+	−	−	+	+
Spring	−	+	+	−	−	+	+	−	−	+	−	+
Summer	+	+	+	−	−	+	−	+	+	−	−	+

5. Discussion

a. Wave and littoral drift regime

Based on the available archive of a Waverider buoy (Araújo et al. 2003) and NWW3 reanalysis of an 11-year time series, the 1997–2007 period (Pianca, Mazzini, and Siegle 2010), various authors have defined the wave climate of the southern Brazilian coast. Swells and winds associated with the passage of cold fronts are the dominant forcing mechanisms.

Strauch et al. (2009) also observed the predominance of waves coming from the east, east-southeast, southeast, and south-southeast from a Waverider anchored between 2006 and 2007 on the northeast RS coast.

Kamphuis (1991), Van Rijn (2001, 2002), and Van Rijn and Boer (2006) analyzed the CERC formula, comparing the estimates with data measured in the laboratory and field, and they concluded that it tends to overestimate longshore transport, especially in storm events. This overestimation could partially explain the higher drift rates obtained with equation (1) when compared with the results from equations (2) and (3).

The reversal of net littoral drift in the midcoast (Fig. 8) is related to the geographic position of extratropical cyclones in the Atlantic Ocean. Parise, Calliari, and Krusche (2009) identified three patterns of cyclone trajectories, one of which is generated on the southern Uruguayan coast with displacement to the east and the resulting east and east-southeast wave propagation (type 2). Littoral drift reversal has been observed in certain years with the predominance of this cyclogenesis pattern. Codignotto et al. (2012), using mathematical models of wave generation and analyzing series from the past 35 years, observed changes in the wave regime in the La Plata River region between Uruguay and Argentina, with an increase in the frequency and height of waves coming from the east and east-southeast. This change may have been associated with an increase in frequency of extratropical cyclones (type 2). Large sets of beach ridges in cells 1 and 2 (Corrêa, Aliotta, and Weschenfelder 2004) are consistent with the process of littoral drift reversal.

b. Sediment budget

A negative residual value was found in the sediment budget. This difference is more than 10 million m^3 using equation (1) and 3.7 and 3.3 million m^3 using equations (2) and (3), respectively. Part of this deficit is caused by the Rio Grande jetties, which prevent the transfer of sediments from the south coast into cell 1, and another cause is sediment transfer from cell 12 toward the north coast. If the Rio Grande jetties did not exist, littoral drift rates to the northeast in the southernmost segment of cell 1 would have reduced the negative residual result to -6.5 million m^3 using equation (1) (Fig. 9) and -1.7 and -1.5 million m^3 using equations (2) and (3), respectively.

Toldo et al. (2006) and Lopes et al. (2008) have observed, through mapping of shoreline mobility and littoral drift estimates, that the midcoast of RS has high rates of erosion, especially in beaches south of Mostardas. These authors have determined that sediments eroded from these locations are deposited in zones with greater shoreline inflection, between the Mostardas and Dunas Altas beaches, in a process that leads to natural beach enlargement caused by the littoral drift jam. Thus, these beach deposits have become an important source of sediment for the dune field.

Geomorphological indicators such as the Conceição lighthouse, located in cell 4; dune field widening between cells 6–8 and 10–12; and geoindicators observed by Corrêa, Aliotta, and Weschenfelder (2004) and Toldo et al. (2006) are consistent with the results obtained in

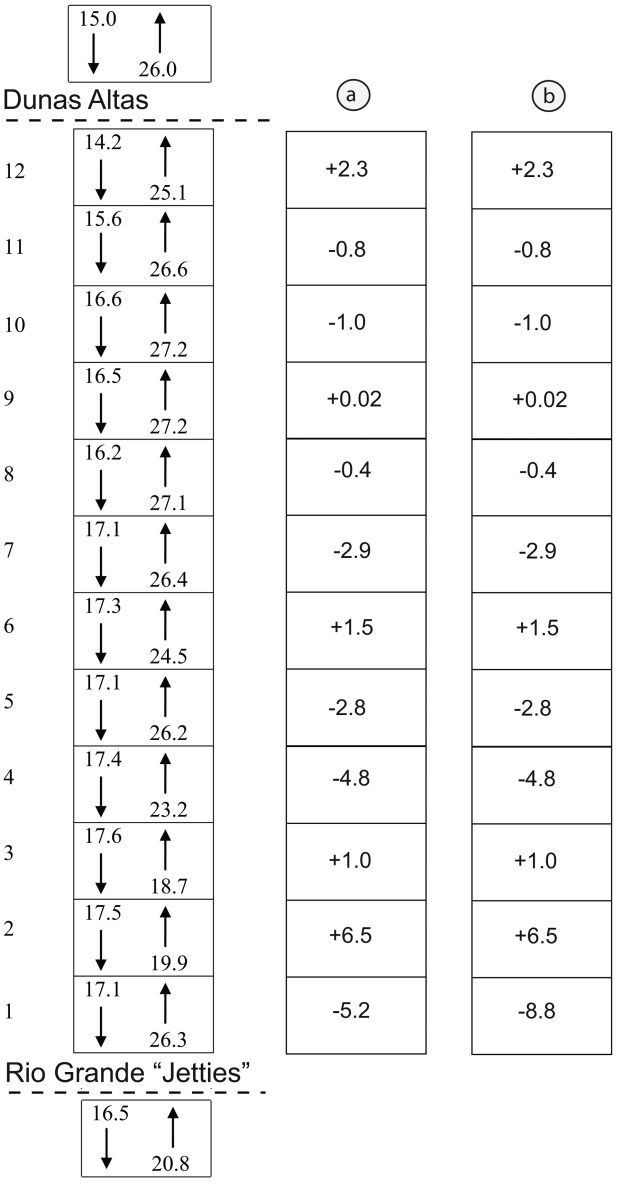

Figure 9. Sediment budget ($\times 10^6$ m^3) by littoral drift rates from equation (1). (a) Historical balance before the jetties, with sediment exchange through the inlet (input of the 20.8×10^6 m^3 from south beaches to cell 1 and output to south of the 17.1×10^6 m^3). (b) After construction of the jetties, without the input of south coast littoral drift.

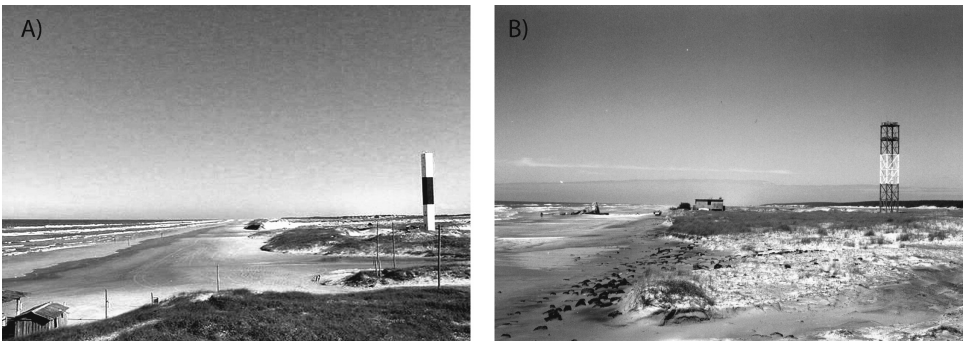

Figure 10. Photographs showing beaches classified as sediment sink and source. (a) Dunas Altas located in cell 12 exemplifies a beach with large sediment deposits on subaerial beach and dune fields. (b) Conceição lighthouse in cell 4 shows the opposite pattern with smaller beach deposits, including the destruction of the lighthouse built in 1922 far from 200 m from the waterline (the old structure was destroyed and a new one built, left and right sides of the picture, respectively).

the sediment budget and respective littoral cell classifications as sediment sources or sinks. Also, the use of other geoindicators such as height of the dune, submarine morphology, and width and slope of the beach allowed us to classify the coastline mobility behavior. The cells classified as sediment sinks are characterized by high frontal dunes reaching 20 m in Dunas Altas, gentle slopes and wide subaerial beaches, and large submerged banks located in the shoreface. On the other hand, cells classified as sediment sources have small or no dunes, and the subaerial beach is narrow and steep (Fig. 10).

c. Sediment dynamics of the RS midcoast

Cell 1, located in the extreme south of the area, is the greatest source of sediments for the other cells, except in the summer, when it acts as a sink because of the net littoral drift reversal to the southwest. Cell 2 is the largest sediment sink and showed depositional behavior from 1998 to 2009. The absence of an extensive dune in this cell is ascribed to its orientation parallel to the predominant northeast wind. Cell 3 also behaved as a sink, except during the fall, when it exhibited erosion. Cells 4 and 5 behaved as sediment sources for the other cells and correspond to sections with the largest eroded volumes. Conceição lighthouse in this region is known to have the highest erosion rates of the midcoast, with an average retreat rate of 3.6 m per year (Barletta and Calliari 2003; Parise, Calliari, and Krusche 2009). Cells 6 and 12 showed deposition throughout the period, serving as a sink for sediments eroded from the cells located farther south.

Cells 7 to 11, located between the Mostardas and Dunas Altas beaches, showed major variability in their classification as sediment sources or sinks according to season. Because of the high oblique angle of the alignment of these beaches in relation to the northeast wind,

they acted as sediment sources to feed the extensive dune field. Cell 7 in the spring months (September to December), cell 8 in the winter (June to September) and summer (December to March) months, cell 9 in the fall (March to June) and summer months, cell 10 in the spring months, and cell 11 in the winter months were classified as sediment sinks, indicating strong seasonality of midcoast sediment dynamics (Table 7). A negative sediment budget (negative residuals of 6.50, 0.17, and 0.15 million m^3 according to the equations) exists even when the physical barrier of the Rio Grande jetties is disregarded. This suggests there is a natural deficit of sediments on the midcoast, which causes the significant shoreline mobility and high erosion rates.

Data obtained also enable an estimate of the sand supply from the beach to the dune field. Thus, if the volume of existing sand in the dune field resulted entirely from the beach system, and if the residual determined in the sediment budget was entirely available for aeolian deposition, then the transported volume and necessary time for the formation of this extensive reservoir of sandy sediments could be found. The sand volume in the dune field (4.20 billion m^3) was divided by the sediment budget residual using equation (1), yielding an estimated annual volume transported by the wind of 0.54 million m^3. The time necessary to generate this reservoir is approximately 7.7 ka. This value is consistent with the estimated age of aeolian deposits of the Holocene barrier (Dillenburg et al. 2006; Martinho, Dillenburg, and Hesp 2008). However, the annual sediment input obtained from equations (2) and (3) is approximately 0.14 million m^3, and these supply rates would require 29 ka for the formation of midcoast dune fields. Consequently, the CERC formula (equation 1) appears to provide sediment transport estimates that most closely equate to field evidence on this coast. However, the discrepancy could also be because of shoreface sand supply, which is probably also a source for the dune field (Dillenburg et al. 2000), so the necessary time to create this reservoir is probably lower.

6. Conclusions

After analyzing the results, we conclude that the coastal dune field volume is 4.20 billion m^3. Approximately 3.57 billion m^3 is located between the two most active shoreline segments, in the Mostardas and Dunas Altas beaches, represented by cells 6 to 12.

Additionally, it was possible to estimate the annual aeolian supply rate of sediments toward this reservoir based on the residual volume of the sediment budget (regarding the immense error margin in such calculations) and sand volume contained in the dune field. Based on this analysis, it is possible to conclude that littoral drift rates obtained from the CERC formula (equation 1) are consistent with a minimum reservoir age of approximately 7.7 ka, without considering sediment input from the shoreface. This shows that littoral drift rates estimated with the CERC formula may be more representative on wave-dominated and dissipative-intermediate beaches such as those of the RS coast of Brazil.

Regional littoral drift is bidirectional, with an alternating direction in most cells, especially those with higher angles. Furthermore, net littoral drift to the southwest was observed in

cells farther south, contrary to the regional pattern in 1998, 2000, 2001, 2004, and 2008. Reversals in net littoral drift are related to long-term coastal processes and are controlled by the regional cyclogenesis.

The classifications of cells 7 to 11, located between the greatest shoreline inflections, changed between the fall, winter, spring, and summer months, demonstrating a strong seasonal control in the midcoast sediment budget. Widening of the beach system and the largest sand volumes in the dune field are observed at these sites, which serve as an important sediment source for the midcoast reservoir.

The residual sediment budget showed that the midcoast is naturally subject to erosion, and building of the Rio Grande jetties accentuated this trend through the interruption of sediment supply from the south coast.

Acknowledgments. This article is dedicated to our dear friend Prof. Luiz Emílio de Sá Brito de Almeida. We pay tribute to this late colleague at the Centro de Estudos de Geologia Costeira e Oceânica, a generous, talented, and friendly person. He will remain a reference as an enthusiastic teacher and researcher in coastal science at the Universidade Federal do Rio Grande do Sul.

Our studies have been supported by Conselho Nacional de Desenvolvimento Científico e Tecnológico, Coordenação de Aperfeiçoamento de Pessoal de Nível Superior, CECO, and Instituto de Geociências/UFRGS.

REFERENCES

Almeida, L. E. S. B., N. M. L. Rosauro, E. E. Toldo Jr., and N. L. S. Gruber. 1999. Avaliação da profundidade de fechamento para o litoral norte do Rio Grande do Sul [Depth of closure avaliation in north coast of Rio Grande do Sul], *in* Anais do Simpósio Brasileiro de Recursos Hídricos 13, Belo Horizonte, MG. Porto Alegre, Rio Grande do Sul, Brazil: Associação Brasileiro de Recursos Hídricos.

Anthony, E. J., S. Vanhee, and M. H. Ruz. 2006. Short-term beach–dune sand budgets on the north sea coast of France: Sand supply from shoreface to dunes, and the role of wind and fetch. Geomorphology, *81*, 316–329.

Araújo, C. E. S., D. Franco, E. Melo, and F. Pimenta. 2003. Wave regime characteristics of the southern Brazilian coast, *in* Proceedings of the Sixth International Conference on Coastal and Port Engineering in Developing Countries, COPEDEC VI, Colombo, Sri Lanka, paper 97. 15. CD-ROM.

Barletta, R. C., and L. J. Calliari. 2003. An assessment of the atmospheric and wave aspects determining beach morphodynamic characteristics along the central coast of RS State, southern Brazil. J. Coastal Res., Spec. Issue, *35*, 300–308.

Bowen, A. J., and D. L. Inman. 1966. Budget of Littoral Sands in the Vicinity of Point Arguello, California. Technical Memorandum No. 19. Washington, DC: U.S. Army Coastal Engineering Research Center, 41 pp.

Calliari, L. J., E. E. Toldo Jr., and J. L. Nicolodi. 2006. Classificação Geomorfológica do Litoral do Rio Grande do Sul, *in* Erosão e Progradação do Litoral Brasileiro, D. Muehe, ed. Brasília, Federal District, Brazil: Ministério do Meio Ambiente, 437–445.

Codignotto, J. O., W. C. Dragani, P. B. Martin, C. G. Simionato, R. A. Medina, and G. Alonso. 2012. Wind-wave climate change and increasing erosion in the outer Río de la Plata, Argentina. Cont. Shelf Res., *38*, 110–116.

Cooper, J. A. G., and O. H. Pilkey. 2004. Longshore drift: Trapped in an expected universe. J. Sediment. Res., *74*, 599–606.

Cooper, N. J., J. M. Hooke, and M. J. Bray. 2001. Predicting coastal evolution using a sediment budget approach: A case study from southern England. Ocean Coastal Manage., *44*, 711–728.

Corrêa, I. C. S. 1996. Les variations du niveau de la mer durant les derniers 17.500 ans BP: l'exemple de la plate-forme continentale du Rio Grande do Sul-Brésil. Mar. Geol., *130*, 163–178.

Corrêa, I. C. S., S. Aliotta, and J. Weschenfelder. 2004. Estrutura e evolução dos cordões arenosos pleistocênicos no canal de acesso da Laguna dos Patos-RS, Brasil [Structure and evolution of pleistocenic beach ridges in the Laguna dos Patos channel, RS, Brasil]. Pesqui. Geocienc., *31*, 69–78.

Dillenburg, S. R., P. S. Roy, P. J. Cowell, and L. J. Tomazelli. 2000. Influence of antecedent topography on coastal evolution as tested by the shoreface translation-barrier model (STM). J. Coastal Res., *16*, 71–81.

Dillenburg, S. R., L. J. Tomazelli, P. A. Hesp, E. G. Barboza, L. C. P. Clerot, and D. B. da Silva. 2006. Stratigraphy and evolution of a prograded transgressive dunefield barrier in southern Brazil. J. Coastal Res., Spec. Issue, *39*, 132–135.

Figueiredo, S. A., and L. J. Calliari. 2006. Washouts in the central and northern littoral of Rio Grande do Sul State, Brazil: Distribution and implications. J. Coastal Res., Spec. Issue, *39*, 366–370.

Frihy, O. E., and K. M. Dewidar. 2003. Patterns of erosion/sedimentation, heavy mineral concentration and grain size to interpret boundaries of littoral sub-cells of the Nile Delta, Egypt. Mar. Geol., *199*, 27–43.

Herbich, J. B. 2000. Handbook of Coastal Engineering. New York: McGraw-Hill, 1152 pp.

Jung, G. B., and E. E. Toldo Jr. 2011. Longshore current vertical profile on a dissipative beach. Rev. Bras. Geofis., *29*, 691–702.

Kamphuis, J. W. 1991. Alongshore sediment transport rate. J. Waterw., Port, Coastal Ocean Eng., *117*, 624–641.

Lima, S. F., L. E. S. B. Almeida, and E. E. Toldo Jr. 2001. Estimativa da capacidade do transporte longitudinal de sedimentos a partir de dados de ondas para a costa do Rio Grande do Sul [Estimate of longshore sediment transport from waves data to the Rio Grande do Sul coast]. Pesqui. Geocienc., *28*, 99–107.

Lopes, C. G., A. Zanatta, E. E. Toldo Jr., and J. C. Nunes. 2008. Mobilidade de curto prazo da linha de praia do Litoral Norte e Médio do RS [Short-term mobility of the north and mid-RS coast shoreline], *in* 44° Congresso Brasileiro de Geologia, Curitiba, PR, vol. 1, 593.

Martinho, C. T., S. R. Dillenburg, and P. A. Hesp. 2008. Mid to late Holocene evolution of transgressive dunefields from the Rio Grande do Sul coast, southern Brazil. Mar. Geol., *256*, 49–64.

Parise, C. K., L. J. Calliari, and N. Krusche. 2009. Extreme storm surges in the south of Brazil: Atmospheric conditions and shore erosion. Braz. J. Oceanogr., *57*, 175–188.

Patsch, K., and G. Griggs. 2008. A sand budget for the Santa Barbara Littoral Cell, California. Mar. Geol., *252*, 50–61.

Pianca, C., P. L. F. Mazzini, and E. Siegle. 2010. Brazilian offshore wave climate based on NWW3 reanalysis. Braz. J. Oceanogr., *58*, 53–70.

Rodríguez, E. L., and R. G. Dean. 2009. A sediment budget analysis and management strategy for Fort Pierce Inlet, Florida. J. Coastal Res., *25*, 870–883.

Rosati, J. D. 2005. Concepts in sediment budgets. J. Coastal Res., *21*, 307–322.

Rosati, J. D., and N. C. Kraus. 2001. Sediment budget analysis system (SBAS). ERDC/CHL CHETN-XIV-3. Vicksburg, MS: U.S. Army Engineer Research and Development Center, 13 pp.

Strauch, J. C., D. C. Cuchiara, E. E. Toldo Jr., and L. E. S. B. Almeida. 2009. O padrão das ondas de verão e outono no litoral sul e norte do Rio Grande do Sul [The wave pattern in summer and autumn for south and north coast of Rio Grande do Sul]. Rev. Bras. Recur. Hídricos, *14*, 29–37.

Toldo, E. E., Jr., S. R. Dillenburg, I. C. S. Corrêa, and L. E. S. B. Almeida. 2000. Holocene sedimentation in Lagoa dos Patos Lagoon, Rio Grande do Sul, Brazil. J. Coastal Res., *16*, 816–822.

Toldo, E. E., Jr., L. M. Motta, L. E. S. B. Almeida, and J. C. R. Nunes. 2013. Large morphological change linked to the sediment budget in the Rio Grande do Sul coast. Proc. Coastal Dyn., *1*, 1687–1696.

Toldo, E. E., Jr., J. L. Nicolodi, L. E. S. B. Almeida, I. C. S. Corrêa, and L. S. Esteves. 2006. Coastal dunes and shoreface width as a function of longshore transport. J. Coastal Res., Spec. Issue, *39*, 390–394.

Tolman, H. L. 1997. User Manual and System Documentation of WAVEWATCH-III Version 1.15. NOAA/NWS/NCEP/OMB Technical Note 151. Washington, DC: U.S. Department of Commerce, National Oceanic and Atmospheric Administration, National Weather Service, National Centers for Environmental Prediction, 97 pp.

Tolman, H. L. 1999. User Manual and System Documentation of WAVEWATCH-III Version 1.18. NOAA/NWS/NCEP/OMB Technical Note 166. Washington, DC: U.S. Department of Commerce, National Oceanic and Atmospheric Administration, National Weather Service, National Centers for Environmental Prediction, 110 pp.Tomazelli, L. J., S. R. Dillenburg, and J. A. Villwock. 2000. Late quaternary geological history of the Rio Grande do Sul coastal plain, southern Brazil. Rev. Bras. Geocienc., *30*, 474–476.

Tomazelli, L. J., J. A. Villwock, S. R. Dillenburg, F. A. Bachi, and B. A. Dehnhardt. 1998. Significance of present-day coastal erosion and marine transgression, Rio Grande do Sul, southern Brazil. An. Acad. Bras. Cienc., *70*, 221–229.

U.S. Army Coastal Engineering Research Center. 1984. Shore Protection Manual, 4th ed., vol. 1. Vicksburg, MS: U.S. Department of the Army, Waterways Experiment Station, Corps of Engineers, Coastal Engineering Research Center, 208 pp.

Van Rijn, L. C. 2001. Longshore Sediment Transport. Report Z3054. Delft, The Netherlands: Delft Hydraulics, 100 pp.

Van Rijn, L. C. 2002. Longshore sand transport, *in* Proceedings of 28th Conference on Coastal Engineering, Wales, United Kingdom, no. 28. Singapore: World Scientific.

Van Rijn, L. C., and S. Boer. 2006. The effects of grain size and bottom slope on sand transport in the coastal zone, *in* Proceedings of 30th Conference on Coastal Engineering, San Diego, California, no. 30. Singapore: World Scientific.

Wright, L. D., and A. D. Short. 1984. Morphodynamic variability of surf zones and beaches: A synthesis. Mar. Geol., *56*, 93–118.

Received: *28 September 2014*; revised: *31 March 2015*.